Theory of Laminar Viscous-Inviscid Interactions in Supersonic Flow

JOHN M. KLINEBERG* AND LESTER LEES†
California Institute of Technology, Pasadena, Calif.

This investigation is concerned with those fluid-mechanical problems in which the pressure distribution is determined by the interaction between an external, supersonic inviscid flow and an inner, laminar viscous layer. The boundary-layer approximations are assumed to remain valid throughout the viscous region, and the integral or moment method of Lees and Reeves, extended to include flows with heat transfer, is used in the analysis. The general features of interacting flows are established, including the important distinctions between subcritical and supercritical viscous layers. The equilibrium solution representing self-induced boundary-layer flow along a semi-infinite flat plate is determined, and a consistent set of departure conditions is derived for determining solutions to interactions caused by external disturbances. Complete viscous-inviscid interactions are discussed in detail, with emphasis on methods of solution for both subcritical and supercritical flows. Results of the present theory are shown to be in good agreement with the measurements of Lewis for boundary-layer separation in adiabatic and nonadiabatic compression corners.

Nomenclature

a = velocity profile parameter, Eqs. (5); also speed of sound
A_1–A_8 = functions defined in Eq. (17)
b = enthalpy profile parameter $(dS/d\eta)_{\eta=0}$, Eq. (6)
B_1–B_8 = functions defined in Eq. (15)
c_v,c_p = specific heats at constant volume and constant pressure
C = $(\mu/\mu_\infty)/(T/T_\infty)$
C_0–C_7 = coefficients of polynomial representations of profile functions
C_f = $2(\mu\partial u/\partial y)_w/\rho_e u_e^2$, skin-friction coefficient
D = determinant of system of equations, Eq. (14)
E = $-\frac{1}{\delta_i^*}\int_0^{\delta_i} S dY$
f = $\left[2 + \frac{\gamma+1}{\gamma-1}\frac{m_e}{1+m_e}\right]\mathcal{K} + \frac{3\gamma-1}{\gamma-1}(1-E) + \frac{M_e^2-1}{m_e(1+m_e)}Z$
F = $\mathcal{K} + [(1+m_e)/m_e](1-E)$
h = function defined in Eq. (16)
h_0 = total enthalpy
$\mathcal{K}$ = θ_i/δ_i^*
J = θ_i^*/δ_i^*
k = thermal conductivity
m = $[(\gamma-1)/2]M^2$; also exponent in similar velocity law
M = Mach number
N_1–N_4 = functions defined in Eq. (14)
p = static pressure
P = $\delta_i^*/U_e(\partial U/\partial Y)_{Y=0}$
P_1–P_4 = perturbation functions defined in Eq. (22)
P_r = Prandtl number $\mu c_p/k$
Q = $\delta_i^*(\partial S/\partial Y)_{Y=0}$
$\bar{Q}$ = Q/P_{r_w}
R = $\frac{2\delta_i^*}{U_e^2}\int_0^{\delta_i}\left(\frac{\partial U}{\partial Y}\right)^2 dY$; also reattachment point
Re_x = $(a_\infty/\nu_\infty)M_\infty x$
$Re_{\delta_i^*}$ = $(a_\infty/\nu_\infty)M_\infty\delta_i^*$ } Reynolds numbers
S = $(h_0/h_{0e}-1)$, total enthalpy function; also separation point
T = static temperature
$T(a,b)$ = $-\int_0^{\eta_{0.99}}\frac{U}{U_e}S d\eta$
T^* = $-\frac{1}{\delta_i^*}\int_0^{\delta_i}\frac{U}{U_e}S dY$
u,v = velocity components parallel and normal to surface
U,V = Stewartson's transformed velocity components
x,y = coordinates parallel and normal to surface
X,Y = Stewartson's transformed coordinates
Z = $\frac{1}{\delta_i^*}\int_0^{\delta_i}\frac{U}{U_e}dY$
$\alpha(a)$ = $\left[\int_0^{\eta_{0.99}}\left(1-\frac{U}{U_e}\right)d\eta\right]^{-1} = \frac{1}{\eta}\frac{Y}{\delta_i^*}$
α_w = inclination of local tangent to surface, measured positive for an expansion turn
β = $(a_e/a_\infty)p_e/p_\infty$
γ = c_p/c_v, ratio of specific heats
δ = boundary-layer thickness
δ_i = transformed boundary-layer thickness
δ_i^* = $\int_0^{\delta_i}\left(1-\frac{U}{U_e}\right)dY$, transformed displacement thickness
ϵ = perturbation parameter
η = $Y\{[(m+1)/2]U_e/\nu_\infty X\}^{1/2}$, Falkner-Skan variable
θ_i = $\int_0^{\delta_i}\frac{U}{U_e}\left(1-\frac{U}{U_e}\right)dY$, transformed momentum thickness
θ_i^* = $\int_0^{\delta_i}\frac{U}{U_e}\left(1-\frac{U^2}{U_e^2}\right)dY$, transformed mechanical energy thickness
Θ = local angle between external streamline at $y=\delta$ and the x axis, $\tan^{-1}(v_e/u_e)$
μ = viscosity coefficient
ν = Prandtl-Meyer angle; also kinematic viscosity μ/ρ
ρ = gas density
σ = $-\int_0^{\eta_{0.99}}S d\eta$
τ = $\mu\partial u/\partial y$, shear stress
τ_k = coefficients for $T(a,b)$, Eq. (7)
$\bar{\chi}$ = $M_\infty^3(C)^{1/2}/(Re_x)^{1/2}$, hypersonic parameter

Subscripts

BL = Blasius point
CR = critical
e,δ = local external, inviscid
i = transformed, incompressible
LE = leading edge

Received September 23, 1968; revision received May 28, 1969. This work was carried out under the sponsorship and with the financial support of the Department of the U.S. Air Force, Air Force Office of Scientific Research under Grant AFOSR-68-1399.

* Research Engineer.
† Professor of Aeronautics. Fellow AIAA.

r = ratio of quantities upstream and downstream of jump
SI = strong interaction
TH = throat conditions
w = wall (surface)
WI = weak interaction
0 = reference conditions
1 = upstream of jump
2 = downstream of jump
$\infty, \infty -$ = freestream conditions upstream of interaction
$\infty +$ = conditions far downstream of interaction

I. Introduction

In the usual formulation of boundary-layer theory, the distribution of static pressure along the surface is determined by the inviscid flow over the body in the absence of a boundary layer. In this sense, the effects produced by the viscous stresses are assumed to result in perturbations on an existing flowfield. There are many important problems in fluid mechanics, however, for which the static pressure distribution cannot be specified in advance but is determined by the interaction between the outer inviscid flow and the inner viscous layer near the surface. One of the most interesting problems of this type is the viscous-inviscid interaction caused by a rise in static pressure in the external supersonic stream. This pressure rise may be generated, for example, by an incident oblique shock or a compression corner, and often induces boundary-layer separation far upstream of the location of the disturbance. This type of interaction, where there is a strong coupling between the outer inviscid flow and the inner boundary layer, requiring the simultaneous development of both solutions, is the subject of the present theoretical investigation.

Because of the complexity of these viscous-inviscid interactions, an integral or moment method is used in the analysis, as discussed in Sec. II. The governing differential equations for adiabatic and nonadiabatic flows are developed in Sec. III, and the nature of the solutions of these equations is discussed in Sec. IV. Section V contains a description of specific methods of solutions for various interactions, whereas the results of some numerical computations are given in Sec. VI.

II. Theoretical Considerations

In the solution of many boundary-layer problems, a method utilizing integral relations is often required. The basic advantage of this approach is that it allows the partial differential equations describing the flow to be integrated across the viscous layer and reduced to ordinary differential equations. Although some of the details of viscous-inviscid interactions cannot be examined in this manner, an integral formulation permits the understanding of many of the important features of the flowfield through a relatively simple analysis of the influence of the main parameters.

In addition to the integrated form of the three conservation equations for mass, momentum, and energy, it is necessary to use at least one moment of the momentum equation in order to avoid the semiempirical features inherent in methods such as the Crocco-Lees[1] mixing theory. This additional equation has been used by Sutton,[2] Walz,[3] Tani,[4] and more recently by Lees and Reeves,[5,6] among others. It is also necessary to couple the viscous and inviscid flows at the boundary-layer edge through a relation between $\Theta(x) = \tan^{-1} v_e/u_e$, the induced inclination of the inviscid streamline at $y = \delta$, and $M_e(x)$, the Mach number at the edge of the viscous layer. The use of this system of equations permits the introduction of four dependent functions to describe the flow: a thickness parameter $\delta_i^*(x)$, the Mach number $M_e(x)$; and two independent profile parameters, $a(x)$ and $b(x)$, to represent the velocity and total enthalpy profiles. The distributions of the dependent quantities as functions of x are determined by the solution of the differential equations subject to the boundary conditions associated with a specific viscous-inviscid interaction.

III. Differential Equations

The basic system of equations consists of the three conservation equations for compressible flow and the equation for the rate of change of mechanical energy, obtained by multiplying the momentum equation by the velocity u. The boundary-layer approximations are assumed to be valid, and the equations are integrated across the viscous layer and transformed into an equivalent incompressible form by means of the Stewartson[7] transformation. The resulting system of four first-order, nonlinear, ordinary differential equations can be written as follows.

Continuity:

$$F\frac{d\delta_i^*}{dx} + \delta_i^*\left[\frac{d\mathcal{H}}{dx} - \frac{1+m_e}{m_e}\frac{dE}{dx}\right] + \delta_i^* f\frac{d\ln M_e}{dx} = \beta\frac{1+m_e}{m_e(1+m_\infty)}\tan\Theta \quad (1)$$

Momentum:

$$\mathcal{H}\frac{d\delta_i^*}{dx} + \delta_i^*\frac{d\mathcal{H}}{dx} + \delta_i^*(2\mathcal{H}+1-E)\times \frac{d\ln M_e}{dx} = \beta C\frac{M_\infty}{M_e}\frac{P}{Re_{\delta_i^*}} \quad (2)$$

Moment of momentum (mechanical energy):

$$J\frac{d\delta_i^*}{dx} + \delta_i^*\frac{dJ}{dx} + \delta_i^*(3J-2T^*)\times \frac{d\ln M_e}{dx} = \beta C\frac{M_\infty}{M_e}\frac{R}{Re_{\delta_i^*}} \quad (3)$$

Energy:

$$T^*\frac{d\delta_i^*}{dx} + \delta_i^*\frac{dT^*}{dx} + \delta_i^* T^*\times \frac{d\ln M_e}{dx} = \beta C\frac{M_\infty}{M_e}\frac{Q}{P_{rw}Re_{\delta_i^*}} \quad (4)$$

This is the minimum number of equations necessary to describe nonadiabatic viscous interactions adequately. Additional moments can be added at the cost of including additional velocity-profile and enthalpy-profile parameters. This increased complexity, however, is not thought worthwhile at the present time, and the simplest possible formulation has been adopted.

A. Velocity and Total Enthalpy Profiles

Many of the difficulties previously encountered in the use of integral methods can be traced to poor or inappropriate profile representation. Lees and Reeves[5] have shown that the solutions of the Falkner-Skan[8] equation for similar flow, including the reversed-flow profiles found by Stewartson,[9] can successfully be used to represent the flow quantities. This approach has been followed here for flows with heat transfer, using the Cohen-Reshotko[10] analogs of Stewartson's solutions in a manner similar to that employed by Holden.[11]

It should be emphasized that the use of similarity solutions to represent profile quantities is entirely different from the assumption of local similarity, where the profile shape is related to the local value of the pressure gradient. The present approach also differs from the method proposed by Thwaites,[12] in which the similar flow solutions are used to correlate a profile-shape parameter and the local skin-friction coefficient as a function of a local pressure-gradient parameter. No dependence between profile shape and local pressure gradient

is assumed in the present analysis, and the similarity solutions are used only to specify relations among the different functions of the velocity and total enthalpy distributions. For example, if two parameters a and b are used to denote the similar velocity and total enthalpy profiles, respectively, functional relations of the form $\mathcal{H} = \mathcal{H}(a)$, $J = J(a)$, $E = E(a,b)$, $T^* = T^*(a,b)$ are required. The distributions of a and b as functions of x are then determined by the solution of the differential equations with appropriate boundary conditions.

Since the Cohen-Reshotko[10] similarity variable η and the Y coordinate are linearly related, i.e., $Y = k\eta$, there is a direct correspondence between the similar profile quantities and the boundary-layer functions appearing in Eqs. (1–4). The transformed displacement thickness, for example, can be written

$$\delta_i^* \equiv \int_0^{\delta_i} \left(1 - \frac{U}{U_e}\right) dY = k \int_0^{\eta(\delta_i)} \left(1 - \frac{U}{U_e}\right) d\eta$$

$$\equiv \frac{k}{\alpha} = \frac{Y}{\alpha\eta}$$

where

$$\alpha = \left[\int_0^{\eta_{0.99}} \left(1 - \frac{U}{U_e}\right) d\eta\right]^{-1}$$

and

$$\eta(\delta_i) = (\eta)_{u/u_e=0.99} \equiv \eta_{0.99}$$

i.e., the edge of the boundary layer is taken at the point where the velocity $u = 0.99u_e$. It should be noted that the choice of edge is not important provided a reasonable boundary between the viscous and inviscid flows is taken. For example, the edge may be defined as the point at which the shear stress is 1% of its peak value, but the definition becomes meaningless if the shear is required to be 0.01% of its maximum. In the moment method, the only function which is sensitive to the choice of edge is the velocity integral Z appearing in the continuity equation.

Using the quantity $\alpha = (1/\eta)Y/\delta_i^*$ as the scaling parameter, all nondimensional profile functions can be obtained from equivalent similarity expressions. For example,

$$\theta_i \equiv \int_0^{\delta_i} \frac{U}{U_e}\left(1 - \frac{U}{U_e}\right) dY = \alpha\delta_i^* \times \int_0^{\eta_{0.99}} \frac{U}{U_e}\left(1 - \frac{U}{U_e}\right) d\eta$$

hence,

$$\mathcal{H} \equiv \frac{\theta_i}{\delta_i^*} = \alpha \int_0^{\eta_{0.99}} \frac{U}{U_e}\left(1 - \frac{U}{U_e}\right) d\eta$$

The two independent parameters used to describe the profile functions can be selected from among the quantities appearing in the similarity solutions, such as $\mathcal{H}$, for example, which remain everywhere single-valued and finite. Following the procedure of Lees and Reeves,[5] the parameter describing the velocity distribution was selected as follows.

Attached velocity profiles $[f''(0) \geq 0]$:

$$a(x) = \eta_{0.99} f''(0) = \left[\frac{\partial(U/U_e)}{\partial(Y/\delta_i)}\right]_{Y=0} \qquad 0 \leq a < 4 \quad (5a)$$

Separated velocity profiles $[f''(0) \leq 0]$:

$$a(x) = \frac{(\eta)_{f'=0}}{\eta_{0.99}} = \left(\frac{Y}{\delta_i}\right)_{U/U_e=0} \qquad 0 \leq a < 1 \quad (5b)$$

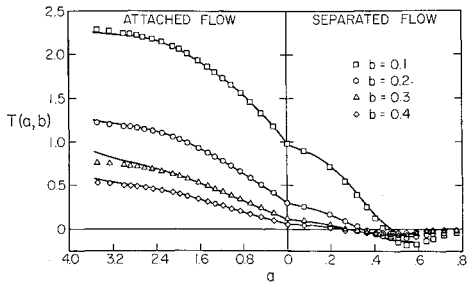

Fig. 1 Theoretical T distributions for flows near a solid surface.

The second parameter was chosen to specify the distribution of total enthalpy as follows:

$$b(x) = S'(0) = \alpha(a)\left[\frac{\partial S}{\partial(Y/\delta_i^*)}\right]_{Y=0} \qquad 0 \leq b < 0.5 \quad (6)$$

When a sufficient number of similarity solutions has been obtained and the required profile quantities tabulated, the easiest procedure is to express these quantities as polynomial functions of the two parameters using a least-squares curve fit. The distributions of integrals which are functions of both a and b can be obtained from the polynomial representation of the quantity $\alpha = \alpha(a)$, and from the integrals

$$\sigma(b) = -\int_0^{\eta_{0.99}} S d\eta \quad \text{and} \quad T(a,b) = -\int_0^{\eta_{0.99}} \frac{U}{U_e} S d\eta$$

where $T(a,b)$ can be expressed in terms of the two parameters as follows:

$$T(a,b) = \sum_{k=0}^{5} \tau_k(b) a^k, \quad \text{where} \quad \tau_k(b) = \sum_{l=0}^{5} D_{kl} b^l \quad (7)$$

The distribution of the quantity $T(a,b)$ is shown in Fig. 1, and the coefficients of the curve fits of all profile functions are given in Tables 1–3.

B. Induced Streamline Inclination Θ

For two-dimensional interactions in which the local external flow can be considered isentropic, the inclination $\Theta = \tan^{-1} v_e/u_e$ of the inviscid streamline at $y = \delta$ can be related to the Mach number at the edge of the viscous layer through the Prandtl-Meyer relation, i.e.,

$$\Theta = \alpha_w(x) + \nu(M_{\infty\pm}) - \nu(M_e) \quad (8)$$

where $\alpha_w(x)$ is the inclination of the local tangent to the surface, considered positive for an expansion turn. The reference condition must be selected such that $M_{\infty\pm}$ is the Mach number which the local external flow either departs from or approaches through an isentropic process.

For certain interactions, particularly in hypersonic flow, a direct relation between Θ and the static pressure ratio may be a better, or more convenient, approximation. In these cases, the tangent-wedge relation is useful, i.e.,

$$\Theta = \alpha_w(x) + \frac{(p_e/p_\infty - 1)}{\gamma M_\infty}\left[1 + \frac{\gamma+1}{2\gamma}\left(\frac{p_e}{p_\infty} - 1\right)\right]^{-1/2} \quad (9)$$

This relation is obtained by examining the oblique shock equations for small deflections and high Mach number and is therefore valid for nonisentropic flows. However, since the Mach number M_e appears directly in the differential equations, the external flow must usually be assumed isentropic. An approximate method for including some of the effects of the entropy variation induced by the curvature of the leading-edge shock is discussed in Ref. 13.

Table 1 Coefficients of functions $\mathfrak{F} = \sum_{k=0}^{7} C_k a^k$ for $S_w = 0$

Fct.	C_0	C_1	C_2	C_3	C_4	C_5	C_6	C_7
				Attached profiles				
$\mathfrak{IC}$	0.24711	0.11056	−0.02122	0.00435	−0.00097	0.000099		
J	0.37372	0.16969	−0.02336	0.00572	−0.00175	0.000191		
Z	1.03539	0.48373	−0.01502	0.02610	−0.00370			
R	1.25782	−0.55550	0.31964	−0.09077	0.01398	−0.000935		
P		0.48745	−0.09927	0.00960	−0.00031			
$d\mathfrak{IC}/da$	0.11056	−0.04245	0.01304	−0.00389	0.00050			
$dJ/d\mathfrak{IC}$	1.50031	0.28105	−0.04287	0.00262				
				Separated profiles				
$\mathfrak{IC}$	0.24711	−0.25057	−0.43012	0.1430	−0.4267	−10.8587	38.7425	−31.209
J	0.37372	−0.42859	0.33036	−5.1517	10.5964	−5.8174		
Z	1.03539	−1.02605	−1.12405	−1.1456	3.3434			
R	1.25782	1.09008	7.01736	−33.8762	196.7688	−371.9762	244.3095	
P		−1.19450	−0.70990	−7.1253	20.8568	−100.2729	310.2394	−263.587
$d\mathfrak{IC}/da$	−0.25057	−0.86024	0.42888	−1.7068	−54.2937	232.4553	−218.4644	
$dJ/d\mathfrak{IC}$	1.50031	−0.84045	3.32376	−13.8668	5.4767	30.1770		

C. Final Form of Differential Equations

Once the functional dependence of the profile quantities with respect to a and b has been determined and either of the relations, Eq. (8) or (9), for the streamline angle Θ is used, the only dependent variables in the differential equations, Eqs. (1–4), are $M_e(x)$, $\delta_i^*(x)$, $a(x)$, and $b(x)$. By regarding the equations as a set of algebraic relations for the four unknown first derivatives and solving simultaneously, the following convenient form for numerical computation is obtained:

$$\frac{\delta_i^*}{M_e}\frac{dM_e}{dx} = \frac{\beta C}{Re_{\delta_i^*}}\frac{M_\infty}{M_e}\frac{N_1(M_e,a,b,h)}{D(M_e,a,b)} \tag{10}$$

$$\frac{d\delta_i^*}{dx} = \frac{\beta C}{Re_{\delta_i^*}}\frac{M_\infty}{M_e}\frac{N_2(M_e,a,b,h)}{D(M_e,a,b)} \tag{11}$$

$$\delta_i^*\frac{da}{dx} = \frac{\beta C}{Re_{\delta_i^*}}\frac{M_\infty}{M_e}\frac{N_3(M_e,a,b,h)}{D(M_e,a,b)} \tag{12}$$

$$\delta_i^*\frac{db}{dx} = \frac{\beta C}{Re_{\delta_i^*}}\frac{M_\infty}{M_e}\frac{N_4(M_e,a,b,h)}{D(M_e,a,b)} \tag{13}$$

where

$$\begin{aligned} D(M_e,a,b) &= B_1\partial T^*/\partial b - B_2\partial F/\partial b \\ N_1(M_e,a,b,h) &= B_3\partial T^*/\partial b - B_4\partial F/\partial b \\ N_2(M_e,a,b,h) &= B_5\partial T^*/\partial b - B_6\partial F/\partial b \\ N_3(M_e,a,b,h) &= B_7\partial T^*/\partial b - B_8\partial F/\partial b \\ N_4(M_e,a,b,h) &= B_4 f + B_6 F + B_8\partial F/\partial a - B_2 h \end{aligned} \tag{14}$$

and

$$\begin{aligned} B_1 &= A_6\partial F/\partial a + (A_3 f - A_8 F)d\mathfrak{IC}/da \\ B_2 &= A_6\partial T^*/\partial a + (A_3 - A_8)T^* d\mathfrak{IC}/da \\ B_3 &= A_2\partial F/\partial a + (A_3 h - A_4 F)d\mathfrak{IC}/da \\ B_4 &= A_2\partial T^*/\partial a + (A_3\bar{Q} - A_4 T^*)d\mathfrak{IC}/da \\ B_5 &= A_7\partial F/\partial a + (A_4 f - A_8 h)d\mathfrak{IC}/da \\ B_6 &= A_7\partial T^*/\partial a + (A_4 T^* - A_8\bar{Q})d\mathfrak{IC}/da \\ B_7 &= A_6 h - (A_2 f + A_7 F) \\ B_8 &= A_6\bar{Q} - (A_2 + A_7)T^* \end{aligned} \tag{15}$$

Table 2 Coefficients of functions $\mathfrak{F} = \sum_{k=0}^{6} C_k a^k$ for $S_w = -0.8$

Fct.	C_0	C_1	C_2	C_3	C_4	C_5	C_6
				Attached profiles			
$\mathfrak{IC}$	0.21360	0.14559	−0.02557	−0.00186	0.001535	−0.000166	
J	0.31943	0.21814	−0.02530	−0.00236	0.000699		
Z	0.85886	0.57514	−0.07002	0.11862	−0.043803	0.004701	
R	1.46008	−0.97913	0.66413	−0.22727	0.040415	−0.002924	
P		0.53307	−0.13418	0.00786	0.004420	−0.000652	
$d\mathfrak{IC}/da$	0.14559	−0.05113	−0.00559	0.00614	−0.000828		
$dJ/d\mathfrak{IC}$	1.47875	0.30409	−0.04296				
α	0.34201	0.27176	−0.17846	0.22393	−0.077497	0.008345	
$d\alpha/da$	0.27176	−0.35692	0.67179	−0.30999	0.041725		
				Separated profiles			
$\mathfrak{IC}$	0.21360	−0.06348	−1.82056	10.5576	−37.0821	57.6139	−31.3578
J	0.31943	−0.19173	−0.86790	3.4359	−15.7682	28.6497	−16.5293
Z	0.85886	−0.55378	−0.28422	−6.2356	12.5892	−6.4777	
R	1.46008	−0.39010	28.23864	−174.5137	579.1440	−831.3955	449.0166
P		−0.67296	1.87130	−18.2666	32.7836	−13.0597	
$d\mathfrak{IC}/da$	−0.14158	−0.73754	−0.63091	6.2296	−66.1475	190.6747	−148.9183
$dJ/d\mathfrak{IC}$	1.47875	−1.08822	6.76658	−27.6252	34.3417		
α	0.34201	−0.16153	−0.66107	0.1122	0.4768		
$d\alpha/da$	−0.16153	−1.32214	0.33669	1.9073			

Table 3 Coefficients of functions $\mathfrak{F} = \sum_{k=0}^{5} C_k b^k$ for $S_w = -0.8$

Fct.	C_0	C_1	C_2	C_3	C_4	C_5
			All profiles			
τ_0	3.83752	−50.4572	298.3153	−931.740	1484.142	−946.400
σ	6.58297	−65.9303	388.3395	−1281.151	2169.799	−1462.240
$d\sigma/db^a$	−67.73754	822.7200	−3964.621	6877.003		
$d\sigma/db^b$	−26.00272	156.8862	−364.054	303.164		
			Attached profiles			
τ_1	1.40078	−5.4123	−5.0795	72.853	−159.677	114.788
τ_2	−0.61326	3.1527	5.2273	−72.156	178.176	−142.029
τ_3	0.27055	−1.4014	−0.7717	27.041	−76.321	66.368
τ_4	−0.07926	0.3459	0.0244	−5.457	16.185	−14.452
τ_5	0.00886	−0.0293	−0.0827	0.993	−2.676	2.312
			Separated profiles			
τ_1	−2.40293	2.6544	106.704	−599.404	1245.35	−922.51
τ_2	9.90203	148.1774	−2296.430	10542.237	−20643.13	14902.15
τ_3	−64.89342	−732.9078	11501.861	−51438.209	98239.36	−69432.32
τ_4	85.64821	1753.8714	−22042.646	91942.596	−168678.92	115980.25
τ_5	−37.67211	−946.2056	10221.085	−38487.998	64640.07	−41071.43

[a] $b \leq 0.2$.
[b] $b \geq 0.2$.

where

$$\frac{\partial F}{\partial a} = \frac{d\mathfrak{K}}{da} - \frac{1 + m_e}{m_e}\frac{\partial E}{\partial a}, \quad \frac{\partial F}{\partial b} = -\frac{1 + m_e}{m_e}\frac{\partial E}{\partial b} \tag{16}$$

$$h = \frac{M_e}{M_\infty}\frac{1 + m_e}{m_e(1 + m_\infty)} Re_{\delta_i^*}\frac{\tan\Theta}{C}$$

and

$$A_1 = 2\mathfrak{K} + 1 - E, \; A_5 = 3J - 2T^*$$
$$A_2 = PJ - \mathfrak{K}R, \; A_6 = A_1 J - A_5\mathfrak{K}$$
$$A_3 = \mathfrak{K}dJ/d\mathfrak{K} - J, \; A_7 = A_1 R - A_5 P \tag{17}$$
$$A_4 = PdJ/d\mathfrak{K} - R, \; A_8 = A_1 dJ/d\mathfrak{K} - A_5$$

For the adiabatic case, Eqs. (14) reduce to the following:

$$D(M_e,a) = A_6 + A_3 f - A_8 F$$
$$N_1(M_e,a,h) = A_2 + A_3 h - A_4 F$$
$$N_2(M_e,a,h) = A_7 + A_4 f - A_8 h$$
$$N_3(M_e,a,h) = (A_6 h - A_2 f - A_7 F)/(d\mathfrak{K}/da)$$

where $E = T^* = 0$ in Eqs. (17).

IV. Nature of Solutions

A. Subcritical and Supercritical Flows

The essential difference between subcritical and supercritical flows is the inherent instability of subcritical boundary layers as opposed to the stable, or relaxing, nature of supercritical flows. At local supersonic speeds, a thickening subcritical boundary layer, for example, produces a rise in pressure in the external stream which causes a still greater thickening of the layer. Also, a thinning subcritical layer produces a negative pressure gradient in the flow direction which leads to additional thinning of the layer. A supercritical boundary layer, on the other hand, cannot generate its own pressure gradient and therefore cannot respond smoothly to a disturbance located downstream. This distinction between subcritical and supercritical flows was first pointed out by Crocco[14] for the case of turbulent boundary layers.

The phenomenon of subcritical-supercritical flows can be demonstrated by integrating the equations for compressible boundary-layer flow to obtain a relation for the induced streamline angle at $y = \delta$ (see Lees[15]). For adiabatic flow, for example,

$$\tan\Theta(\delta) = \frac{1}{\gamma p}\frac{dp}{dx}\left\{\int_0^\delta \left(1 - \frac{\tau_y}{p_x}\right) \times \left(\frac{1 - M^2}{M^2}\right) dy\right\} + \frac{\gamma}{2} M_e^2 C_f \tag{18}$$

where $M^2 = u^2/a^2$.‡ Now, on the scale of disturbance of particular interest here, the first term on the right-hand side of the previous equation is much larger than the second term. For hypersonic flow, where $\tan\Theta(\delta) \simeq d\delta/dx$, Eq. (18) shows that the sign of $d\delta/dp$ depends on the sign of the integral. For a flat plate, for example, $(1 - \tau_y/p_x) \geq 0$; hence, the sign of the integral depends on the behavior of the quantity $(1 - M^2)/M^2$ across the viscous layer. If the subsonic portion of the boundary layer is sufficiently large, $d\delta/dp > 0$ and the viscous layer is subcritical. On the other hand, if the subsonic region is small, $d\delta/dp < 0$ and the viscous layer is supercritical. In fact, a detailed analysis (see Lees,[15] Garvine,[16] and Section V.A of this paper) shows that the pressure and boundary-layer thickness diverge initially from the equilibrium strong-to-weak interaction at an exponential rate when the layer is subcritical. If the flow is supercritical, however, the viscous layer always returns to the equilibrium solution when perturbed slightly.

B. Subcritical-Supercritical Transition

In the moment method formulation, the simultaneous vanishing of the determinant D and the numerators N, Eqs. (14), describes a locus of singular points at which the derivatives dM_e/dx, da/dx, etc. are not single-valued. It is this locus of singularities of the system of equations which marks the transition between subcritical and supercritical flows.

For adiabatic boundary layers, the points $D = 0$ prescribe a unique relationship between M_e and a, as shown in Fig. 2. In this case, the critical points $D = 0$ lie in the region $a >$

‡ The integrand in this equation remains finite near $y = 0$ since $(p_x - \tau_y) \sim u^2$ near the wall.

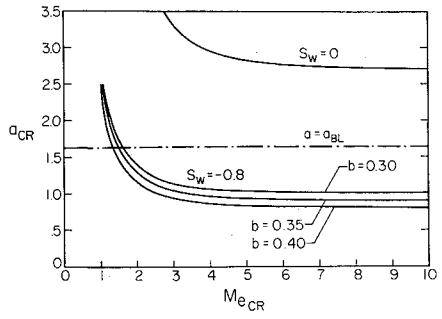

Fig. 2 Locus of critical points for $S_w = 0$ and $S_w = -0.8$.

a_{BL}, corresponding to velocity profiles that have been accelerated above the zero pressure-gradient solution, e.g., flow in an expansion turn. Self-induced viscous flow along a flat plate and interactions caused by compressive disturbances are therefore always subcritical in adiabatic flow, and $D \neq 0$ everywhere in the interaction region.

For nonadiabatic boundary layers, the locus of critical points $D = 0$ describe a surface which is a function of M_e, a, and b. In highly cooled ($S_w = -0.8$) flow, the critical points for $M_e > 2$ lie in the region $a < a_{BL}$, Fig. 2, corresponding to velocity profiles between the separation and flat-plate solutions. Viscous flow along a highly cooled surface is therefore supercritical unless there is a compressive disturbance which decelerates the flow toward separation. If such a disturbance is present, the boundary layer must undergo a transition from a supercritical to a subcritical state at some location upstream of the disturbance.

In the moment method formulation, the condition for continuous transition between subcritical and supercritical flows is given by the requirement for the numerators N_1, N_2, N_3, and N_4 in Eqs. (10–13) to vanish when $D = 0$. It is sufficient, however, for only one of the numerators to vanish at the critical point since the N's are obtained from the same set of equations and thus are not all independent. The relation for the singular point, or throat, can thus be written

$$h_{TH} = \left\{\left[\left(A_4F\frac{d\mathcal{H}}{da} - A_2\frac{\partial F}{\partial a}\right)\frac{\partial T^*}{\partial b} + B_4\frac{\partial F}{\partial b}\right]\Big/\left[A_3\frac{d\mathcal{H}}{da}\frac{\partial T^*}{\partial b}\right]\right\}_{D=0} \quad (19)$$

For adiabatic flow, this reduces to the simple expression

$$h_{TH} = [(A_4F - A_2)/A_3]_{D=0}$$

One result to be obtained from these equations is the required sign of the induced streamline inclination Θ at the throat. For adiabatic flow, for example, $h_{TH} > 0$; hence, the angle Θ must be positive at the critical point to allow the boundary layer to pass through the singularity. Using the Prandtl-Meyer relation, Eq. (8), this means that transition can only occur along a surface for which

$$\alpha_w(x) > \nu(M_e) - \nu(M_{\infty\pm}) \quad (20)$$

Since the adiabatic boundary layer must be accelerated in order to become supercritical, $M_e > M_{\infty-}$ and the right-hand side of the previous inequality is positive. Smooth subcritical-supercritical transition is therefore possible for adiabatic flow in an expansion turn provided the throat is located along the curved portion of the body [$\alpha_w(x) > 0$].

The inequality given in Eq. (20) also indicates a second possibility for smooth transition in adiabatic flow. For a supercritical boundary layer expanding toward a downstream Blasius condition, such that $M_e < M_{\infty-}$, smooth transition from a supercritical to a subcritical state can occur along a flat surface. This situation can arise for flow along an adiabatic flat plate downstream of either a blunt leading edge or an expansion corner in which the boundary layer becomes supercritical.

For highly cooled ($S_w = -0.8$) flow at moderately supersonic Mach numbers ($M_e > 2$), the induced angle Θ must be negative at the throat. Smooth transition is therefore possible provided

$$\alpha_w(x) < \nu(M_e) - \nu(M_{\infty\pm}) \quad (21)$$

Since nonadiabatic flat-plate flow is initially supercritical, Eq. (21) indicates that continuous supercritical-subcritical transition is not possible on a flat surface upstream of a compressive disturbance ($M_e < M_{\infty-}$). Although the inequality implies that smooth transition might occur in a gradual compression turn [$\alpha_w(x) < 0$], such particular solutions are of little practical interest. In highly cooled flows, therefore, the viscous-inviscid interaction caused by a compressive disturbance cannot occur smoothly, but must be initiated by a discontinuous transition, or jump, to a subcritical state at some point upstream of the disturbance. The jump, of course, is an approximation to the actual transition from supercritical to subcritical flow occurring over one or two boundary-layer thicknesses (see Sec. V.B). The boundary layer downstream of the jump remains subcritical through the interaction region and can return to a supercritical state far downstream of the disturbance, where $M_e > M_{\infty+}$ and smooth transition along a flat surface is possible.

C. Solutions in the Phase Space

An understanding of some of the aspects of viscous-inviscid interactions can be obtained from an analysis of the behavior of integral curves in the $Re_{\delta i}{}^* - a - M_e$ phase space. For adiabatic flow, the critical points $D = 0$ define a cylindrical surface in the phase space parallel to the $Re_{\delta i}{}^*$ axis dividing the domain into subcritical and supercritical regions. At a given reference Mach number, the singular points $N_i = D = 0$, Eq. (14), describe a line on this surface for each value of $\alpha_w(x)$. For the special case of flat-plate flow [$\alpha_w(x) = 0$], the locus of singularities represents the intersection of the critical surface with the surface containing the Blasius point at downstream infinity. This second surface has been called the "relaxation surface" by Tyson,[17] who demonstrated numerically that all integral paths which relax to the Blasius condition lie in this surface. By using the proper form of the moment equations, the relaxation surface can be extended to include the leading-edge singularity and thus contains the

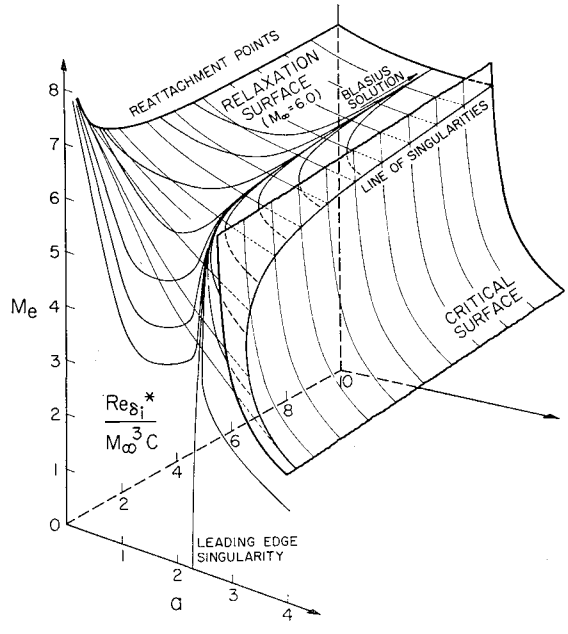

Fig. 3 Phase-space geometry for adiabatic flow.

complete equilibrium solution for undisturbed viscous flow over a semi-infinite flat plate. With this consideration, the geometry of the phase space for adiabatic flow is shown in Fig. 3.

The existence of the relaxation surface is very important in the analysis of viscous-inviscid interactions. Only those integral paths that lie in the relaxation surface can decay toward the downstream Blasius condition, while all other solutions diverge away from the surface. The diverging solutions, or departure integrals, correspond to flow upstream of some disturbance, whereas solutions in the relaxation surface represent flow downstream of a disturbance. In the supercritical portion of the phase space, on the other hand, all integral paths converge toward the singular line; hence there are no departure integrals. These flows can respond to a downstream disturbance only through a jump from the solution in the supercritical region to the corresponding subcritical departure integral. In the absence of external disturbances, however, the solution curves pass continuously into the relaxation surface on the subcritical side. The locus of singularities $N_i = D = 0$ is therefore a line of nodal points for all supercritical-subcritical trajectories, and at every singular point there is one exceptional nodal path that remains in the relaxation surface. All other integral curves leave the relaxation surface in response to some downstream disturbance.

The analysis of trajectories in the phase space indicates an important numerical procedure for obtaining solutions to many viscous-inviscid interactions. Since all departure integrals diverge away from the relaxation surface in the downstream direction, any perturbation of a solution lying in the surface will generate a departure integral. As a result, it is difficult to obtain an integral curve remaining in the relaxation surface, particularly if the solution approaches the line of singularities. Integration in the upstream direction is stable, however, since in this manner the departure integral passing through any point in the phase space can be traced back to its origin on the relaxation surface. For many interactions, it is necessary to determine the downstream, or relaxing, portion of the solution by integrating away from the Blasius point corresponding to the final freestream Mach number. The complete solution can be determined by matching the upstream and downstream branches of the integral curve at some intermediate point. The method of iterating for the correct trajectory in the relaxation surface is described in Sec. V.C.

For highly cooled ($S_w = -0.8$) flows, the Blasius point lies in the supercritical portion of the phase space. The relaxation surface therefore contains those subcritical integral curves that converge toward the line of singularities, since these are the only trajectories that can relax to a downstream Blasius condition. All solutions in the supercritical region decay toward the Blasius point, and there are no departure integrals in this portion of the phase space. Supercritical-subcritical transition on a highly cooled flat plate therefore always takes place through a discontinuity, or jump, in the flow quantities. The location of the jump is determined by the condition that the subcritical branch of the solution downstream of the disturbance must lie in the relaxation surface corresponding to $M_{\infty+}$ and subsequently pass through the critical surface at the singular line.

V. Methods of Solution

A. Departure Conditions for Subcritical Flows

As indicated in Sec. IV, a small perturbation of any of the integral paths lying in the relaxation surface generates a departure solution on integration in the downstream direction. If the initial point in the relaxation surface lies along the trajectory passing through the leading-edge singularity, the departure integrals form a single-parameter family of

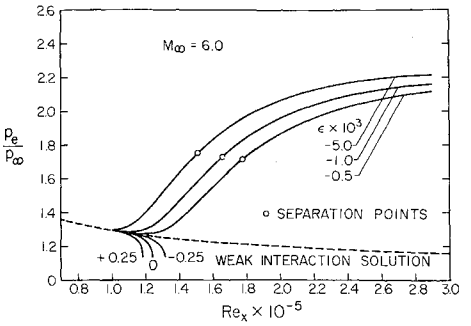

Fig. 4 Effect of ϵ on adiabatic free interaction.

solutions which can be described, for example, by the extent of departure from any fixed point in the surface. This family contains those integral paths usually referred to as "free-interaction" solutions. The parameter describing the departure distance can be determined by linearizing the equations about any point along the eigensolution representing undisturbed flat-plate flow.

Ko and Kubota[18] have performed this linearization for adiabatic flow in the vicinity of the Blasius solution, using the hypersonic form of the moment equations. The method of analysis used is completely general, however, and the results are valid for all initial points except those in the immediate neighborhood of the leading edge, where the surface derivatives are of the same order as the departure derivatives. The required perturbations for adiabatic and slightly cooled subcritical flows are of the form

$$M_e = M_{e0}(1 + P_1\epsilon),\ \delta_i^* = \delta_{i0}^*(1 + P_2\epsilon)$$
$$a = a_0(1 + P_3\epsilon),\ b = b_0(1 + P_4\epsilon) \tag{22}$$

where

$$P_1 = [\mathfrak{C}dJ/d\mathfrak{C} - J]$$
$$P_2 = [3J - 2T^* - (2\mathfrak{C} + 1 - E)dJ/d\mathfrak{C}]$$
$$P_3 = [(2\mathfrak{C} + 1 - E)J - (3J - 2T^*)\mathfrak{C}]/[d\mathfrak{C}/da]$$
$$P_4 = [(P_1 + P_2)T^* + P_3\partial T^*/\partial a]/[\partial T^*/\partial b]$$

The effect of the perturbation quantity ϵ on the static pressure ratio upstream of a disturbance in adiabatic flow is shown in Fig. 4. The integral path $\epsilon = 0$ does not correspond exactly to the unperturbed eigensolution because the weak-interaction expansion used in the computation places the initial point slightly off the relaxation surface. In general, however, $\epsilon < 0$ generates the family of solutions going toward separation, whereas $\epsilon > 0$ gives trajectories corresponding to flow upstream of an expansion corner. As can be seen from Fig. 4, the length scale for accelerating boundary layers is much shorter than the scale for separating flows.

B. Departure Conditions for Supercritical Flows

For highly cooled flat-plate flows, there are no departure solutions in the sense of the previous section since the flow is supercritical and all perturbations decay exponentially in the downstream direction. In the present method, the transition from supercritical to subcritical flow is regarded as discontinuous, and jumps in the fluxes of mass, momentum, and mechanical energy are allowed. As previously indicated, the requirement for a jump arises from the fact that the actual transition from supercritical to subcritical flow occurs over one or two boundary-layer thicknesses. This scale of disturbance is much less than the length scale of interest in the present analysis, and the rapid change in flow quantities in the transition region is approximated by a discontinuity. In order to eliminate the need for a jump, it would be necessary to include terms from the Navier-Stokes

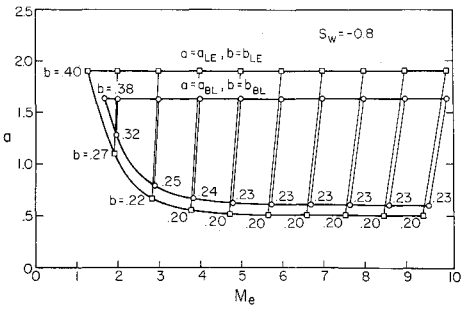

Fig. 5 Locus of jumps from Blasius and leading-edge solutions.

equations which are neglected in the boundary-layer approximation, and, in particular, to allow for pressure variations in the normal direction. There is a close analogy between this situation and the ordinary shock wave in "inviscid" gas dynamics, where the effects of viscosity and heat conduction are confined to a narrow region and the Eulerian equations are retained to describe the flowfield.

In the moment method, since the supercritical flow upstream of the jump is characterized by four quantities, M_e, δ_i^*, a, and b, four equations are required to determine the downstream conditions uniquely. These jump relations, which are discussed in Ref. 19, can be written in the form

$$m_{e_2}F_2\left[\frac{\mathfrak{IC}_1}{m_{e_1}F_1} - \frac{\mathfrak{IC}_2}{m_{e_2}F_2}\right] + \frac{1}{\gamma M_{e_1}^2}\left(\frac{p_2}{p_1} - 1\right)[m_{e_2}F_2 + Z_2] - (1 - \rho_r u_r^2)(Z_2 - \mathfrak{IC}_2) + (1 - \rho_r u_r)\left(1 + \frac{\mathfrak{IC}_1}{m_{e_1}F_1}\right)Z_2 = 0 \tag{23}$$

$$m_{e_2}F_2\left[\frac{J_1}{m_{e_1}F_1} - \frac{J_2}{m_{e_2}F_2}\right] + \frac{2u_r}{\gamma M_{e_1}^2}\left(\frac{p_2}{p_1} - 1\right) \times [m_{e_2}J_2 + Z_2 - (1 + m_{e_2})T_2^*] - (1 - \rho_r u_r^3)(Z_2 - J_2) + (1 - \rho_r u_r)\left(1 + \frac{J_1}{m_{e_1}F_1}\right)Z_2 = 0$$

$$m_{e_2}F_2\left[\frac{T_1^*}{m_{e_1}F_1} - \frac{T_2^*}{m_{e_2}F_2}\right] + (1 - \rho_r u_r)\left(T_2^* + \frac{T_1^*}{m_{e_1}F_1}Z_2\right) = 0$$

and

$$\frac{M_r\delta_r^*}{\rho_r u_r} = \frac{m_{e_1}F_1}{m_{e_2}F_2 + (1 - \rho_r u_r)Z_2}$$

where the subscript r denotes the ratio of quantities upstream and downstream of the jump, i.e.,

$$M_r = \frac{M_{e_2}}{M_{e_1}},\ \delta_r^* = \frac{\delta_{i_2}^*}{\delta_{i_1}^*},\ \rho_r u_r = \frac{\rho_{e_2}u_{e_2}}{\rho_{e_1}u_{e_1}}$$

The pressure and density ratios can be determined from the change in Mach number M_e by means of the oblique shock relations, and the first three equations can be solved for a_2, b_2, and M_{e_2} for any given upstream conditions. The change in the transformed displacement thickness can then be obtained from the last equation. Some typical jumps from the Blasius and strong-interaction solutions for highly cooled ($S_w = -0.8$) flow are shown in Fig. 5.

The subcritical flow downstream of the jump generates a pressure gradient along the surface which produces separation and the beginning of a region of reversed flow. The departure integrals, consisting of the jump and the interacting boundary layer upstream of the disturbance, form a one-parameter family of solutions for initial states corresponding to flat-plate flow. Thus as a given disturbance moves toward the leading edge, the boundary layer upstream of the jump becomes more supercritical, the strength of the jump increases and the separation point approaches the jump location. For supercritical as well as subcritical flows, the correct departure integral is always determined by the downstream boundary condition appropriate to the specific viscous-inviscid interaction considered.

C. Downstream Solutions

As previously indicated, it is often necessary to obtain the downstream portion of a particular solution by integrating away from the Blasius point corresponding to the final freestream Mach number. It is not possible to integrate the equations toward the leading edge in the physical space, however, because the weak-interaction solution is obtained in the asymptotic limit $\bar{\chi} \to 0$ and the value of the Reynolds number Re_x at the starting point is therefore not determined within a small constant. The integration must be performed in the phase space by iterating for the initial conditions in the vicinity of the Blasius point which generate the required trajectory.

The correct method of iteration for adiabatic flow is given by an analysis by Ko and Kubota[18] of the singular point at downstream infinity. Their results indicate that solutions in the relaxation surface can be determined by selecting initial values for integration in the upstream direction such that

$$M_e = M_{eWI} + \Delta M_e,\ Re_{\delta i^*} = (Re_{\delta i^*})_{WI},\ a = a_{WI} + \Delta a \tag{24}$$

where

$$\Delta a = \frac{4}{(\gamma - 1)^2}\left[\frac{(dP/da)(dJ/d\mathfrak{IC}) - dR/da}{J - \mathfrak{IC}dJ/d\mathfrak{IC}} - \frac{dP}{da}\right]_{BL}^{-1} \times \left(\frac{Re_{\delta i^*}}{M_\infty{}^3C}\right)_{WI}\left(\frac{\Delta M_e}{M_\infty}\right) \approx -5.63\left(\frac{Re_{\delta i^*}}{M_\infty{}^3C}\right)_{WI}\left(\frac{\Delta M_e}{M_\infty}\right)$$

Here the subscript WI refers to the eigensolution for $\bar{\chi} \ll 1$ corresponding to the freestream Mach number, pressure, density, and velocity far downstream of the interaction. The starting values are iterated according to Eq. (24) until the integral path which joins the upstream branch of the solution is obtained. The result can be transformed into physical coordinates by quadrature, and from the value of Re_x at the joining point the downstream solution can be located in the physical space. Some of the trajectories in the relaxation surface determined by this iteration procedure are shown in Fig. 3.

For many interactions it may not be possible to assume that the body extends far enough downstream for the effect of the trailing edge to be neglected. In supercritical flow, if the trailing edge is located downstream of the critical point, the solution is independent of the length of the body. In subcritical flow, however, the effect of finite length is communicated upstream into the interaction region. For configurations for which there is a rapid expansion of the flow at the trailing edge, however, the boundary layer must become supercritical and $D \to 0$ at this location. The beginning of the interaction and the magnitude of the perturbation ϵ for these finite-length bodies may therefore be determined such that $D = 0$ at the given location of the trailing edge (see Ko and Kubota[18]).

VI. Numerical Results

A. Hypersonic Flow over a Semi-Infinite Flat Plate

For all sharp-nosed bodies in the absence of external disturbances, the flowfield can be divided asymptotically into two regions, the strong- and weak-interaction zones. Because of the singular nature of the solutions in these two regions, asymptotic expansions for the flow variables can be obtained for the interactions in both limits. In the strong-

interaction region, for example, a coordinate expansion in large $\bar{\chi}$ for the pressure ratio yields

$$(p_e/p_\infty)_{SI} = A_0\bar{\chi}[1 + A_1(\bar{\chi})^{-1} + A_2(\bar{\chi})^{-2} + \ldots]$$

whereas in the weak-interaction region, the pressure ratio is of the form

$$(p_e/p_\infty)_{WI} = 1 + a_1\bar{\chi} + a_2\bar{\chi}^2 + \ldots$$

The coefficients for these expansions are given in Refs. 13 and 20 (see also Kubota and Ko,[21] for adiabatic weak-interaction results). The complete solution for undisturbed flat-plate flow can be determined, once the asymptotic expansions have been obtained, by integrating the differential equations in the intermediate region.

For an adiabatic surface, the eigensolution for self-induced flow lies in the subcritical portion of the phase space, and the integral path originating at the leading edge must be obtained by integrating upstream, away from the Blasius point. Using the iteration procedure described in Sec. V.C, the correct trajectory is matched to the strong-interaction expansion to determine the initial value of Re_x, and from this the solution can be located in the physical space. The result of this iteration for the pressure distribution is shown in Fig. 6.

For highly cooled ($S_w = -0.8$) flat-plate flow, integration in the downstream direction is stable and the solution in the intermediate region can be obtained directly. Using initial conditions given by the strong-interaction expansion, the set of differential equations can be integrated away from the leading edge in the physical space. The result of this integration for the pressure distribution is shown in Fig. 6.

Because of viscous dissipation in the boundary layer, the effect of any external disturbance can be considered negligible at some point upstream of the location of the disturbance. The results discussed previously, therefore, not only give a solution to the classical problem of hypersonic viscous flow over a semi-infinite flat plate, but also provide the locus of approximate initial states for other viscous-inviscid interactions. The solution for the interaction caused by a given external disturbance is obtained by applying the proper departure conditions to the eigensolution for self-induced flow at a location where the effects of the external disturbance are small. The correct location for the beginning of the interaction is the one that generates a solution satisfying the geometric constraints and boundary conditions associated with a particular viscous-inviscid interaction.

B. Interactions Generated by Incident Shock Waves

In the analysis of boundary-layer/shock-wave interactions, the velocity profile, enthalpy profile, transformed displacement thickness, and static pressure ratio are taken to be continuous at the shock-impingement location. The angle Θ, however, is discontinuous because the flow at the boundary-layer edge is turned through both the incident shock and the reflected expansion fan. Since far from the body shock reflection from the viscous layer is identical with reflection from a solid boundary, the downstream Mach number, $M_{\infty+}$, can be taken to be the Mach number behind the reflected shock which turns the inviscid flow parallel to the surface. The induced streamline inclination Θ downstream of impingement can therefore be determined from the values of $M_{\infty+}$ and M_e, the edge Mach number calculated from the static pressure at impingement, and from the entropy change across the incident shock. Thus for a given shock strength, all conditions immediately downstream of the point of incidence are uniquely determined from the viscous flow upstream of impingement.

In most interactions caused by incident shock waves, both the location of impingement and the strength of the shock are specified for a particular problem. As a result, an iterative procedure must be used to obtain a solution satisfying the required conditions. For adiabatic or slightly cooled subcritical flows, the Reynolds number Re_{x_0} denoting the be-

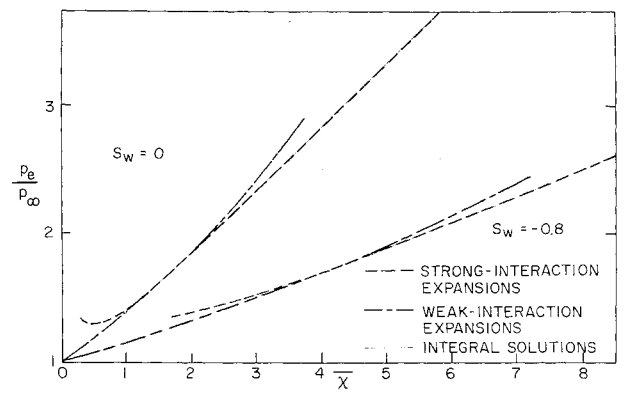

Fig. 6 Hypersonic flat-plate pressure distributions for adiabatic and nonadiabatic flows.

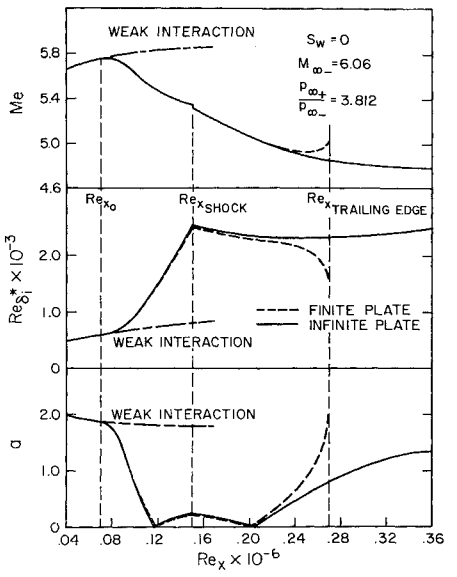

Fig. 7 Trajectories for adiabatic boundary-layer/shock-wave interaction.

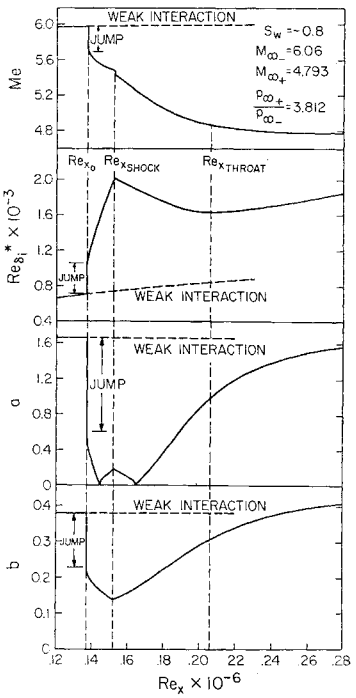

Fig. 8 Trajectories for nonadiabatic boundary-layer/shock-wave interaction.

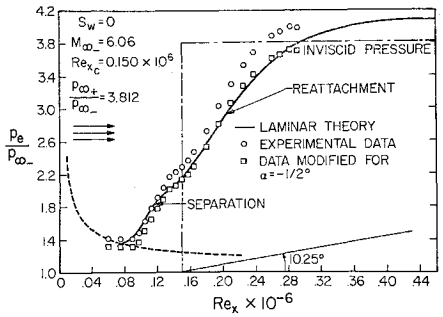

Fig. 9 Experimental and theoretical pressure distributions for adiabatic flow.

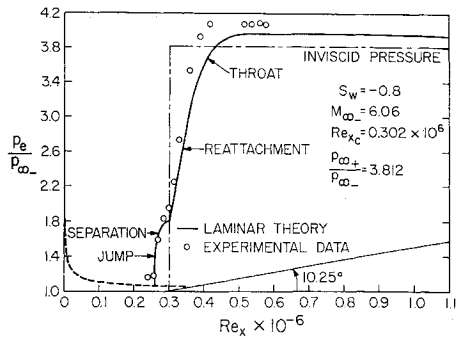

Fig. 11 Experimental and theoretical pressure distributions for nonadiabatic flow.

ginning of the interaction must be selected far upstream of the point of incidence. A departure integral leaving the eigensolution for undisturbed flow and proceeding toward separation can be obtained by applying a small negative value of the perturbation parameter ϵ to the viscous flow at that location (see Fig. 4). Integration of the equations is continued smoothly through separation to the point of shock impingement, where, as discussed previously, new initial conditions for the integral path downstream of the incident shock are determined. If the subsequent trajectory does not approach the downstream boundary conditions, the assumed value for Re_{x_0} must be modified and the entire procedure repeated. When the approximately correct integral curve has been obtained, it is convenient to iterate for the perturbation quantity ϵ in order to determine the exact solution. As a general rule, $0 < |\epsilon| < |\epsilon_{\max}|$ where $\epsilon_{\max}$ is the value of the perturbation parameter which gives $dM_e/dx = 0$ at the beginning of the interaction.

The results of a typical computation for adiabatic flow are shown in Fig. 7. The two solutions represent interactions beginning in the weak-interaction zone for both a finite ($D \to 0$ at the trailing edge) and a semi-infinite ($N_1, N_3 \to 0$ as $Re_x \to \infty$) flat plate. It is evident that a small change in the value of ϵ can generate very different integral curves because of the high degree of nonlinearity of the equations in the subcritical region.

For nonadiabatic supercritical flows, the interaction caused by an incident shock wave must be initiated by a jump to a subcritical state at some point upstream of the location of impingement. The correct jump location is determined by the requirement for smooth subcritical-supercritical transition downstream of reattachment. The method of solution is similar to the one used for subcritical flows except that there is only one iteration parameter, the Reynolds number Re_{x_0} denoting the beginning of the interaction and the location of the jump.

The results of a typical computation for highly cooled ($S_w = -0.8$) flow at the same freestream conditions as the previous adiabatic interaction are shown in Fig. 8. Since the throat is a true saddle-point singularity for the system of differential equations, it is not possible to obtain a numerical solution passing continuously from the subcritical to the supercritical region. An effective procedure is to iterate for the correct jump location Re_{x_0} and then to modify slightly either the strength of the incident shock or the point of impingement in order to extend the integral curve in the downstream direction. When the location of the throat has been determined as precisely as possible, the solution in the subcritical region can be graphically extrapolated through the singularity into the supercritical region. Downstream of this point the equations are stable and the integration proceeds smoothly toward the Blasius condition at infinity.

Figures 9–11 show comparisons of the theory for boundary-layer/shock-wave interactions with several experimental pressure distributions obtained by Lewis[22] for flow in sharp compression corners. As indicated by Reeves,[23] the two flowfields are similar provided $Re_{x_{\text{corner}}} = Re_{x_{\text{shock}}}$ and the total pressure ratio $p_{\infty+}/p_{\infty-}$ is identical. The agreement shown between theory and experiment is quite good, particularly since the measured value of the freestream pressure $p_{\infty-}$ represents an approximate quantity.[24] If the effect of even a very small flow inclination on the surface pressures is included, i.e., if the plate is assumed to be at an angle of attack $\alpha = -\frac{1}{2}°$, the small systematic discrepancies between theory and experiment disappear and the agreement is extremely good (Fig. 9).

The result of cooling the surface can be seen from a comparison of the previous figures. The most dramatic effect of surface temperature is the marked change in the over-all length of the interaction. For example, if the region of influence of the incident shock is considered to extend downstream to the point where $M_e = M_{\infty+}$, the length of the interaction in highly cooled ($S_w = -0.8$) flow is reduced to 40% of the length of the corresponding adiabatic interaction.

Figure 12 shows the pressure distributions for two interactions occurring close to the plate leading edge in highly cooled ($S_w = -0.8$) flow. The computations correspond to ramp angles of 22.5° and 27.5° at a freestream Mach number $M_{\infty-} = 16.0$. These conditions are similar to those investi-

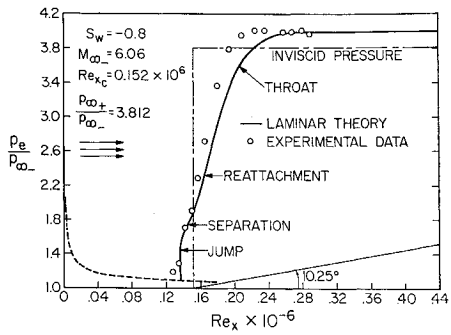

Fig. 10 Experimental and theoretical pressure distributions for nonadiabatic flow.

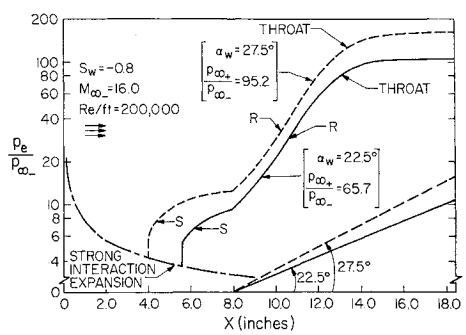

Fig. 12 Effect of disturbance strength in nonadiabatic flow.

gated by Miller, Hijman, and Childs,[25] although the nonisentropic effects caused by the curvature of the leading-edge shock must be included in the calculations if a direct comparison between theory and experiment is to be made.

References

[1] Crocco, L. and Lees, L., "A Mixing Theory for the Interaction between Dissipative Flows and Nearly Isentropic Streams," *Journal of the Aerospace Sciences*, Vol. 19, 1952, pp. 649–676.

[2] Sutton, W. G. L., "An Approximate Solution of the Boundary Layer Equations for a Flat Plate," *Philosophical Magazine*, Vol. 23, 1937, pp. 1146–1152.

[3] Walz, A., "Anwendung des Energiesatzes von Wieghardt auf einparametrige Geschwindingkeitsprofile in laminaren Grenzschichten," *Ingenieur-Archiv*, Vol. 16, 1948, pp. 243–248.

[4] Tani, I., "On the Approximate Solution of the Laminar Boundary Equations," *Journal of the Aeronautical Sciences*, Vol. 21, 1954, pp. 487–504.

[5] Lees, L. and Reeves, B. L., "Supersonic Separated and Reattaching Laminar Flows: I. General Theory and Application to Adiabatic Boundary-Layer/Shock-Wave Interactions," *AIAA Journal*, Vol. 2, No. 11, Nov. 1964, pp. 1907–1920.

[6] Reeves, B. L. and Lees, L., "Theory of the Laminar Near Wake of Blunt Bodies in Hypersonic Flow," *AIAA Journal*, Vol. 3, No. 11, Nov. 1965, pp. 2061–2074.

[7] Stewartson, K., "Correlated Incompressible and Compressible Boundary Layers," *Proceedings of the Royal Society (London), Ser. A*, Vol. 200, No. A1060, 1949, pp. 84–100.

[8] Falkner, V. M. and Skan, S. N., "Some Approximate Solutions of the Boundary Layer Equations," RM 1314, 1930, British Air Research Council.

[9] Stewartson, K., "Further Solutions of the Falkner-Skan Equation," *Proceedings of the Cambridge Philosophical Society*, Vol. 50, 1954, pp. 454–465.

[10] Cohen, C. B. and Reshotko, E., "Similar Solutions for the Compressible Laminar Boundary Layer with Heat Transfer and Pressure Gradient," Rept. 1293, 1956, NACA.

[11] Holden, M. S., "An Analytical Study of Separated Flows Induced by Shock Wave-Boundary Layer Interaction," Rept. AI-1972-A-3, 1965, Cornell Aeronautical Lab.

[12] Thwaites, B., "Approximate Calculation of the Laminar Boundary Layer," *Aeronautical Quarterly*, Vol. 1, Nov. 1949, pp. 245–280.

[13] Klineberg, J. M., "Theory of Laminar Viscous-Inviscid Interactions in Supersonic Flow," Ph.D. thesis, 1968, California Inst. of Technology, Pasadena, Calif.

[14] Crocco, L., "Considerations on the Shock-Boundary Layer Interaction," *Proceedings of the Conference on High-Speed Aeronautics*, Polytechnic Inst. of Brooklyn, Jan. 1955, pp. 75–112.

[15] Lees, L., "Viscous-Inviscid Flow Interactions at Supersonic Speeds," First Annual Dean's Lecture, University of Notre Dame, April 10–11, 1967.

[16] Garvine, R. W., "Upstream Influence in Viscous Interaction Problems," *The Physics of Fluids*, Vol. 11, No. 7, July 1968, pp. 1413–1423.

[17] Tyson, T. J., "Laminar Boundary Layers in the Neighborhood of Abrupt Spatial Disturbances," Ph.D. thesis, 1967, California Inst. of Technology, Pasadena, Calif.

[18] Ko, D. R. S. and Kubota, T., "Supersonic Laminar Boundary Layer along a Two-Dimensional Adiabatic Curved Ramp," *AIAA Journal*, Vol. 7, No. 2, Feb. 1969, pp. 298–304.

[19] Grange, J. M., Klineberg, J. M., and Lees, L., "Laminar Boundary-Layer Separation and Near-Wake Flow for a Smooth Blunt Body at Supersonic and Hypersonic Speeds," *AIAA Journal*, Vol. 5, No. 6, June 1967, pp. 1089–1096.

[20] Klineberg, J. M. and Lees, L., "Theory of Laminar Viscous-Inviscid Interactions in Supersonic Flow," AIAA Paper 69-7, New York, 1969.

[21] Kubota, T. and Ko, D. R. S., "A Second-Order Weak Interaction Expansion for Moderately Hypersonic Flow past a Flat Plate," *AIAA Journal*, Vol. 5, No. 10, Oct. 1967, pp. 1915–1917.

[22] Lewis, J. E., Kubota, T., and Lees, L., "Experimental Investigation of Supersonic Laminar, Two-Dimensional Boundary-Layer Separation on a Compression Corner with and without Cooling," *AIAA Journal*, Vol. 6, No. 1, Jan. 1968, pp. 7–14.

[23] Reeves, B. L., "The Compressible Boundary Layer in Separated Flow Past a Compression Corner," Report, May 1963, Space General Corp.

[24] Lewis, private communication.

[25] Miller, D. S., Hijman, R., and Childs, M. E., "Mach 8 to 22 Studies of Flow Separations Due to Deflected Control Surfaces," *AIAA Journal*, Vol. 2, No. 2, Feb. 1964, pp. 312–321.